HHS Public Access
Author manuscript
Circulation. Author manuscript; available in PMC 2025 July 23.

Published in final edited form as:
Circulation. 2024 July 23; 150(4): 302–316. doi:10.1161/CIRCULATIONAHA.123.065304.

Deficiency Of the Deubiquitinase, UCHL1, Attenuates Pulmonary Arterial Hypertension

Haiyang Tang, PhD[1,*], Akash Gupta, PhD[2,*], Seth A. Morrisroe[3], Changlei Bao, PhD[1,4], Tae-Hwi Schwantes-An, PhD[5], Geetanjali Gupta, PhD[2], Shuxin Liang, PhD[1], Yanan Sun, PhD[4], Aiai Chu, MD PhD[6], Ang Luo, PhD[4,7], Venkateswaran Ramamoorthi Elangovan, PhD[8], Shreya Sangam, PhD[3], Yinan Shi, PhD[3,4], Samisubbu R. Naidu, PhD[3], Jia-Rong Jheng, PhD[9], Sultan Ciftci-Yilmaz, PhD[3], Noel A. Warfel, PhD[2], Louise Hecker, PhD[10], Sumegha Mitra, PhD[11], Anna W. Coleman[12], Katie A. Lutz[12], Michael W. Pauciulo[12], Yen-Chun Lai, PhD[9], Ali Javaheri, MD PhD[13], Rohan Dharmakumar, PhD[3], Wen-Hui Wu, MD

Correspondence to: Ankit A. Desai, MD, Associate Professor of Medicine, Krannert Institute of Cardiology, Indiana University, 950 West Walnut Street, Building R3, Room #433, Indianapolis, IN 46202, ankdesai@iu.edu.
*Contributed equally

Author Contributions:
HT - contributed to the concept of this study, data collection, drafting of the manuscript, and data analysis; listed first as a co-first author because he contributed a larger proportion of data/manuscript writing than AG
AG - contributed to the concept of this study, data collection, drafting of the manuscript, and data analysis; contributed to all data collection for terminal hemodynamic measurements, provided critical samples, and contributed to writing of the manuscript
SM - contributed to the concept of this study, data collection, drafting of the manuscript, and data analysis
CB - contributed to data analysis and drafting of the manuscript
TSA - contributed to data analysis and drafting of the manuscript
GG - contributed to data collection
SL - contributed to data collection
YS - contributed to data collection
AC – contributed to data collection
AL - contributed to data collection
VE - contributed to data collection
SS - contributed to data collection
YS - contributed to data collection
SRN- contributed to data collection
JJ - contributed to data collection
GH - contributed to data collection
SC - contributed to the data collection
NAW - contributed to the drafting of the manuscript
LH - contributed to the drafting of the manuscript
SM - contributed to the drafting of the manuscript
AC - contributed to the data collection
KL- contributed to the data collection
MWP - contributed to the data collection
YL - contributed to the data collection and drafting of the manuscript
AJ - contributed to the drafting of the manuscript
RD- contributed to the drafting of the manuscript
WHW - contributed to the data collection and drafting of the manuscript
DHP- contributed to the drafting of the manuscript
JHK-- contributed to the data collection
SB - contributed to the data collection and drafting of the manuscript
OB - contributed to the data collection and drafting of the manuscript
SB - contributed to the data collection and drafting of the manuscript
JXY - contributed to the data collection and drafting of the manuscript
JJ - contributed to the drafting of the manuscript
JDD - contributed to data analysis and drafting of the manuscript
WCN - contributed to the data collection and drafting of the manuscript
JGG - contributed to the data collection and drafting of the manuscript
AAD - contributed to the concept and design of this study, data collection, drafting of the manuscript, and data analysis.

Author Conflicts of Interest: The authors have declared that no conflict of interest exists.

PhD[14], **Daniel P Flaherty, PhD**[15], **Jason H Karnes, PhD PharmD**[16], **Sandra Breuils-Bonnet, MSc**[14], **Olivier Boucherat, PhD**[14], **Sebastien Bonnet, PhD**[14], **Jason X-J Yuan, MD PhD**[17], **Jeffrey R Jacobson, MD**[18], **Julio D Duarte, Pharm D PhD**[19], **William C Nichols, PhD**[12], **Joe GN Garcia, MD**[20], **Ankit A. Desai, MD**[3]

[1]State Key Laboratory of Respiratory Disease, National Clinical Research Center for Respiratory Disease, Guangzhou Institute of Respiratory Health, The First Affiliated Hospital of Guangzhou Medical University, Guangzhou, Guangdong, China

[2]Department of Medicine and Arizona Health Sciences Center, Department of Cellular and Molecular Medicine, College of Medicine-Tucson, University of Arizona, Tucson, AZ

[3]Krannert Cardiovascular Research Center, Department of Medicine, Indiana University, Indianapolis, IN

[4]College of Veterinary Medicine, Northwest A & F University, Yangling, China

[5]Department of Medical & Molecular Genetics, Indiana University, Indianapolis, IN

[6]Department of Echocardiography, Gansu Provincial Hospital, Lanzhou, China

[7]Institute of Zoology, Guangdong Academy of Sciences, Guangzhou, China

[8]Department of Pediatrics, University of Michigan, Ann Arbor, MI

[9]Division of Pulmonary, Critical Care, Sleep and Occupational Medicine, Department of Medicine, Indiana University, Indianapolis, IN

[10]Department of Medicine, Emory University, and Atlanta VA Healthcare System, Atlanta, GA

[11]Department of Obstetrics & Gynecology, Indiana University, Indianapolis, IN

[12]Division of Human Genetics, Cincinnati Children's Hospital Medical Center, Department of Pediatrics, University of Cincinnati College of Medicine, Cincinnati, OH

[13]Department of Medicine, Washington University and John Cochran VA Hospital, St. Louis, MO

[14]Department of Medicine, Institut Universitaire de Cardiologie et de Pneumologie de Québec, Université Laval, Quebec, CA

[15]Department of Medicinal Chemistry and Molecular Pharmcacology, Purdue University, Lafayette, IN

[16]Department of Pharmacy Practice and Science, R Ken Coit College of Pharmacy, University of Arizona, Tucson, AZ

[17]Department of Medicine, University of California, San Diego, La Jolla, CA

[18]Department of Medicine, University of Illinois at Chicago, Chicago, IL

[19]Center for Pharmacogenomics and Precision Medicine, Department of Pharmacotherapy and Translational Research, University of Florida, Gainesville, FL

[20]The Herbert Wertheim UF Scripps Institute for Biomedical Innovation and Technology, University of Florida, Jupiter, FL

Abstract

Rationale: While the ubiquitin-proteasome system regulates protein degradation and the development of pulmonary arterial hypertension (PAH), limited is known about the role of deubiquitinating enzymes (DUBs) in this process. Ubiquitin carboxyl-terminal esterase-L1 (UCHL1), a deubiquitinase, has been shown to reduce Akt1 degradation, resulting in higher levels. Given Akt1 is pathological in pulmonary hypertension (PH), we hypothesized that UCHL1 deficiency attenuates PAH development via reductions in Akt1.

Methods/Results: Tissues from animal PH models as well as human PA endothelial cells (HPAECs) from patients with PAH exhibited increased vascular UCHL1 staining and protein expression. Exposure to LDN57444, a UCHL1-specific inhibitor, reduced HPAEC and smooth muscle cell proliferation. Across three pre-clinical PAH models, LDN57444-exposed animals, Uchl1 knockout ($Uchl1^{-/-}$) rats and conditional Uchl1 knockout mice ($Tie2Cre\text{-}Uchl1^{fl/fl}$) demonstrated reduced right ventricular (RV) hypertrophy, RV systolic pressures, and obliterative vascular remodeling. Lungs and PAECs isolated from $Uchl1^{-/-}$ animals exhibited reduced total and activated Akt with increased ubiquitinated Akt levels. UCHL1-silenced HPAECs displayed reduced lysine(K)63-linked and increased K48-linked Akt1 levels. Supporting experimental data, we found that rs9321, a variant in a GC-enriched region of the *UCHL1* gene, is associated with reduced methylation (n=5133), increased *UCHL1* gene expression in lungs (n=815) and reduced cardiac index in patients (n=796). Additionally, growth arrest and DNA damage-inducible alpha gene knockout ($Gadd45\alpha^{-/-}$) mice (established demethylating gene) exhibited reduced lung vascular Uchl1 and Akt1 expression along with attenuated hypoxic PH.

Conclusions: Our findings suggest that UCHL1 deficiency results in PAH attenuation via reduced Akt1, highlighting a novel therapeutic pathway in PAH.

Keywords

Pulmonary arterial hypertension; Uchl1; Ubiquitination

INTRODUCTION

Pulmonary arterial hypertension (PAH) is a rare condition characterized by gradual occlusion of the small pulmonary arterioles, leading to progressively increased pulmonary vascular resistance (PVR) right ventricular (RV) failure and eventual death. Despite advances in management, the long-term prognosis for PAH remains poor [1, 2]. While heritable mutations exhibit reduced penetrance, the variable expressivity, female predominance, and other genetic associations suggest that additional factors modify disease risk and progression [3–6]. Although causal mechanisms of PAH remain largely unclear, histopathology analyses have revealed remodeling across all three layers of the vessel wall (intima, media, adventitia) with uncontrolled hyperplasia in pulmonary artery smooth muscle (PASMCs) and endothelial cells (PAECs) [3, 4, 7–9].

The pathological involvement of Akt1 in driving the hyper-proliferative state of the lung vasculature in PAH is well-established [10, 11]. However, therapeutic studies, primarily from the cancer literature, have mainly focused on inhibiting Akt expression and/or activation, neglecting to explore pathways promoting its degradation [12–14]. Ubiquitination, a reversible post-translational protein modification, regulates protein degradation and membrane trafficking. Deubiquitinases (DUBs) are enzymes responsible for cleaving ubiquitin from the modified proteins. Recent studies have highlighted the role of DUBs in regulating Akt1 protein levels and subsequent activity. Pharmacological inhibition of ubiquitin carboxyl terminal hydrolase 1 (UCHL1), a well- established DUB, resulted in reduced Akt1 protein proteasomal degradation in mice with acute lung injury [15]. Furthermore, reduced growth arrest and DNA damage-inducible alpha (*GADD45α*), an established demethylation gene [15–18], led to reduced UCHL1 and Akt1 expression levels associated with site-specific *UCHL1* promoter methylation.

No prior studies, however have evaluated UCHL1-mediated Akt deubiquitination as a potential mechanism that contributes to the pathogenesis of PAH. The current study rigorously evaluates the role of UCHL1-mediated Akt deubiquitination using several approaches, including epigenetic depletion of *Uchl1* through *Gadd45α* deficiency, pharmacological inhibition, and genetic ablation in animal models of PH. Cumulatively, these findings support the novel role of UCHL1 in the pathogenesis of PAH.

METHODS

Patient cohorts.

Patients with Group 1 PAH defined by right heart catheterization measurements including mean pulmonary artery pressure (mean PAP) ≥ 25 mmHg, pulmonary capillary wedge pressure (PCWP) ≤ 15 mmHg, and pulmonary vascular resistance (PVR) ≥ 3 Woods Units were included in all cohorts. All patients were prospectively recruited for participation in the respective study in accordance with institutional guidelines.

A. University of Arizona (UA) cohort and plasma UCHL1 levels.—Patients with PAH receiving their care at the UA Pulmonary Hypertension clinic between 2012 and 2016 were prospectively enrolled. All participants provided informed consent. The cohort was composed of 94 subjects with Group 1 PAH, including connective tissue disease-associated (n=32), anorexigen/drug-associated (n=6), congenital-associated (n=13), HIV-associated (n=2), portopulmonary (n=6), heritable (n=3), and idiopathic PAH (n=32). For each subject, demographics and clinical testing data were collected, including data from right heart catheterization (RHC), acquired during their first visit (or as part of their initial collections). Plasma collection was performed during consent/enrollment in an outpatient setting. The time between RHC date and enrollment was a mean 1 year, standard deviation of 1.4 years, a median of 0.33 years and 1st quartile at 0 years and 3rd quartile at 1.6 years. Plasma UCHL1 was measured using a commercially available ELISA kit (Antibodies-online.com, Limerick, PA).

Statistical Analysis for UA Cohort.

Hemodynamic measures of PAH severity were compared to plasma UCHL1 protein levels. A multivariable linear regression model was used to test for association between hemodynamic measures to log-transformed plasma UCHL1 protein levels in the UA cohort. We adjusted for age and sex. All analyses were conducted in R version 3.6.0

B. PAH Biobank and *UCHL1* genetics.—Target *UCHL1* single-nucleotide polymorphism (SNP) association analyses were performed using a previously published cohort from the National Biological Sample and Data Repository for Pulmonary Arterial Hypertension (PAH Biobank, www.pahbiobank.org) described in detail in prior reports [5, 19]. Eligible cases were recruited from pulmonary hypertension centers across the United States and Canada and prospectively recruited between October 3, 2012, to March 14, 2016.

Statistical Analysis for PAH Biobank.

Cardiac index (along with other hemodynamic measurements derived from diagnostic RHC) of European ancestry samples and additively coded genotypes for rs9321 (coded for the number of T alleles) were tested for association using linear regression while adjusting for age at PAH diagnosis, sex, and first 10 principal components. Patients with known mutations in *BMPR2* gene were excluded. Genotype data was cleaned as previously described [5, 19]. All analyses were completed in R version 3.6.0.

C. Patient Lung Staining.—Paraffin-embedded sections of lung tissue from subjects with Group 1 PAH and control lungs (died of other non-lung related causes) were obtained from the Department of Pathology, the University of Arizona after approval by the University of Arizona Institutional Review Board.

D. Human PAECs.—PAECs were acquired from the Pulmonary Hypertension Breakthrough Initiative (PHBI). PAECs were isolated and cultured from patients with PAH and control subjects (failed donor lungs). The methods for acquiring the PAECs have previously been detailed [20].

E. RV tissues from patients.—RV tissue acquisition has previously been detailed [21]. All patients provided consent and the protocol for tissue collection was approved by Laval University and the IUCPQ Biosafety and Ethics Committees (CER#20773, CER#20735 and CER#21747). RV samples were categorized as control RV (NRV), compensated RV, and those from subjects with PAH with decompensated RV (dRV) function based on both clinical history and cardiac index (CI) values as previously detailed [21]. Control RVs were obtained from patients with normal RV function who underwent aortic valve surgery or from early autopsies following sudden death for which the previous medical history and the autopsy did not reveal cardiac or respiratory diseases. Compensated RVs were obtained from cardiac biopsies or autopsies of patients with RV hypertrophy and preserved CI (>2.2 L/min/m^2) measured by echocardiography. Decompensated RVs were obtained from early autopsies of patients with end-stage PAH.

Rodent PH models.

All experimental protocols were approved by the Animal Care and Use Committee of the University of Arizona and Indiana University, and the Ethics Committee of the First Affiliated Hospital of Guangzhou Medical University.

A. Mice.—Adult male C57BL/6N or *Gadd45α*$^{-/-}$ mice (8–12 weeks in age, obtained from NCI) were used for all experiments. We used Cre-Lox technology to generate a conditional knockout mouse line with a similar strategy to previous study [22]. Floxed *Uchl1* mice, herein called *Uchl1*$^{flox/flox}$, were purchased from Cyagen Biotechnology (Guangzhou, China) and then were crossed with *Tie2*Cre mice (Cyagen Biotechnology, Guangzhou) for two generations to create *Uchl1*^{Tie2} mice (*Tie2*Cre-*Uchl*$^{flox/flox}$ or *tCre*$^{+}$*Uchl*$^{fl/fl}$). Exposure to normoxia (Nor) and chronic hypoxia (Hyp) for 4–5 weeks (n=6–10) was used as a model for murine PH as previously described [23]. LDN57444 injections (0.5mg/kg/day, IP, dissolved in 2% DMSO) were administered daily for the last two weeks of murine experiments. Strategy for the generation of knockout mice and more detailed Methods and Materials sections are provided in Supplemental Methods.

B. Rats.—In initial experiments, Sprague-Dawley male rats (200 g, n=6–8) were given either a single dose of monocrotaline (MCT) injection (60 mg /kg) or a single dose of SU5416 (20 mg/kg, Cayman Chemical, Ann Arbor, MI). For the MCT-PH model, at the end of 4 weeks, hemodynamic, histologic, and molecular assessments were completed. LDN57444 injections were administered daily starting at week 3 (0.5 mg/kg/day, IP) versus vehicle (Veh) in a subset of rats. For the hypoxia-SU5416-induced PH model (SuHx), rats were placed under hypoxic conditions (FiO_2 10%) for 3 weeks and then were transitioned to normoxia for 4 weeks. LDN57444 injections were administered daily starting at week 4 (0.5 mg/kg/day, IP) versus vehicle in a subset of rats. Additional details on terminal measurements are provided in the Supplemental Methods.

RV tissues from both MCT-exposed rats and the pulmonary artery banding (PAB)-induced RV failure model have previously been described [21]. Briefly, between weeks 1 and 5 following MCT injection or at the end of protocol, rats underwent closed-chest right heart catheterization to measure RV systolic pressure (RVSP), RV end-diastolic pressure (RVEDP), and RV cardiac output, as previously described. Rats were categorized into cRV and dRV according to cardiac output (CO), RVEDP and clinical RV failure signs as previously described [21]. For PAB model, male Sprague-Dawley rats (200 g) were randomized into two groups: sham (Sham) or PAB. PAB Rats were categorized into cRV and dRV according to clinical RV failure signs. Briefly, PAB rats without clinical RV failure signs were categorized as cRV. dRV was applied to PAB rats demonstrating an end-stage of RV failure sign [21].

C. *Uchl1* Knockout Rats (*Uchl1*$^{-/-}$).—Systemic *Uchl1* gene deletion was achieved using Crisper/Cas9 editing in SD rats (Cyagen). Further details provided in Supplemental Methods and Figures S1–S6 as well as Tables S1 and S2. *Uchl1*$^{-/-}$ rats were administered MCT (60 mg/kg) at younger ages, starting at 4 weeks of age for both males and females. Hemodynamic, histologic, and molecular assessments were completed at the end of 3 weeks and compared to cage controls. However, the protocol had to be deviated due to manifestation of progressive and rapid neuromuscular weakness, starting at 7–8 weeks of life. This phenotype was consistent with published genetic mouse models of systemic *Uchl1* deficiency [24–26]. RV histology, endothelial cell isolation, proliferation and tube formation assay were performed as described in the Supplemental Materials.

Statistical analysis.

Values were expressed as means ± SE. Intergroup differences were determined by the student's unpaired *t*-test, while multiple group differences were assessed by a simple ANOVA. *Post hoc* Tukey analysis was used for multiple-comparison test. A value of $P \leq 0.05$ was considered statistically significant (GraphPad Software, San Diego, CA).

The remainder details of Methods are provided in the Supplemental Materials.

RESULTS

UCHL1 expression profiling.

Expression levels of UCHL1 were compared between control and PAH tissues. In patient lung samples, lung vascular UCHL1 staining was stronger in patients with PAH compared to non-PAH controls and was prominent in the endothelial (vWF co-staining) and adventitia layers (Figures 1A and 1B, Figure S7A). In isolated human PAECs, UCHL1 levels were increased in subjects with PAH compared to non-PAH controls (Figure 1C). Similarly, UCHL1 levels were higher in hypertrophied RV samples (cRV combined with dRV samples) compared to those from control subjects (Figure 1D, quantified in Figure S7B). The variation in UCHL1 expression may partly reflect the various patient confounders such as treatment differences, co-morbidities, diet differences, among others that were not available to analyze in our limited cohort along with differences in vascular UCHL1 expression within RV tissues. Immunofluorescence imaging also revealed vascular UCHL1 staining in the RV tissues from a patient sample (Figure S7C).

Western blots revealed elevated UCHL1 and GADD45α levels in whole lungs of rats exposed to MCT and SuHx (Figure 1E) compared to their respective controls. In experimental models of PH, immunohistochemistry of rat lungs from rodent PH models demonstrated similar lung vascular-specific increases in UCHL1 staining compared to controls (Figure 1F). Western blots revealed significantly elevated levels of UCHL1 in RV tissues from cRV and dRV groups of both MCT- and PAB-exposed rats compared to their respective controls (Figure 1G, Figures S7D–7E).

UCHL1 regulates PAEC/SMC proliferation.

To investigate the functional role of UCHL1 in PAH, targeted inhibition of UCHL1 activity with LDN57444 was utilized *in vitro* first in human PAECs. While UCHL1 inhibition did not influence baseline PAEC proliferation, administration of LDN57444 significantly reduced VEGF-induced EC counts and proliferation (Figure 2A and Figure S8A). In parallel, BrdU incorporation in HPAECs were also increased in presence of VEGF and was blocked significantly (Figure 2A) by LDN57444.

Additional evidence of the role of UCHL1 was next demonstrated with a co-culture assay using HPAEC, and human pulmonary artery SMCs (HPASMCs). HPAECs exposed to LDN57444 (Figure 2B, Figure S8B–D) exhibited significantly suppressed VEGF-induced tube formation due to formation of lower numbers of node, junction, and intervals observed in 3D culture along with segments. HPAECs and HPASMCs were next used to investigate how SMC function is regulated by EC after LDN57444 exposure. As expected, VEGF treatment increased HPASMC proliferation co-cultured with PAEC, and exposure to LDN5744 attenuated the proliferative and migratory phenotype (Figure S8E). Cumulatively, these data demonstrate the anti-proliferative properties of UCHL1 inhibition in pulmonary vascular cells after exposure to VEGF.

Uchl1 regulates Akt1 in experimental PH.

To determine mechanistic contributions of UCHL1 inhibition via LDN57444, total and activated Akt1 protein levels were assessed based on prior work [27]. Chronic hypoxic exposure of mouse lungs up-regulated phospho-Akt protein levels with slight increases in total Akt1 levels in whole lungs of wild-type (WT) mice. With Uchl1 inhibition, both total and phospho-Akt protein levels were reduced under normoxia and chronic hypoxia (Figure 2C). Consistent with pharmacological inhibition of Uchl1 in mice, *Uchl1*$^{-/-}$ mutant rats and *Tie2Cre-Uchl1*$^{fl/fl}$ mice exhibited reduced total and phospho-Akt levels in whole lung homogenates compared to controls (Figure 2D–E).

Pharmacological inhibition of Uchl1 attenuates murine PH.

To determine the role of Uchl1 inhibition *in vivo*, a conventional 4-week hypoxic murine PH model was assessed. LDN57444 (vs vehicle) administration during the final two weeks to WT mice resulted in significantly reduced RVSP, ($p<0.0001$, Figure S9A–B) and RVH ($p<0.0001$, Figure S9C) in WT mice. Histologic examination of the lungs revealed that WT mice exposed to LDN57444 demonstrated a reduced pulmonary artery medial thickness index (Figures S9D) compared to vehicle controls when exposed to hypoxia.

Pharmacological inhibition of Uchl1 attenuates rat PH models.

Further potential benefits of UCHL1 inhibition in PAH were supported by the use of the MCT and SuHx rodent models of PH. Similar to mice, the rats with LDN57444 administration in the last two weeks of MCT-injection or in the last 4 normoxic weeks of SuHx-exposure displayed significantly lower RVSP ($p<0.001$), RVH ($p<0.01$), reduction in medial wall thickness and reduced percent obliterated vessel count ($p<0.01$, Supplementary Figures 10A–F) compared to vehicle controls. Additionally, LDN57444 administration significantly reduced cell proliferation within small pulmonary arterioles in sugen-hypoxia-exposed rats as demonstrated by alpha-smooth muscle actin and Ki-67 staining (Supplementary Figure 11).

Uchl1 genetic deletion attenuates rodent PH.

Consistent with murine genetic models of *Uchl1* deficiency [28, 29], systemic deletion of the *Uchl1* gene in rats, at baseline, exhibited significant and progressive neuromuscular weakness. Subtle leg weakness was evident at 6 weeks of age (reduced rodent movement) with complete paralysis manifested by 7–8 weeks of age. By 9 weeks of age, no rats survived. In the modified MCT protocol, exposure to MCT resulted in severe PAH in 3 weeks while *Uchl1*$^{-/-}$ rats displayed reduced RVSP ($p<0.05$), RVH ($p<0.001$) (Figure 3A), muscularized vessel staining and counts (Figures 3B–D), as well as medial wall thickness (p<0.001, Figures 3C), compared to WT. Additionally, Ki67 staining revealed significantly decreased cell proliferation within small pulmonary arterioles in *Uchl1*$^{-/-}$ rats (Figure 3D).

To examine the role of endothelial UCHL1 in the development of hypoxia-induced murine PH, we generated conditional *Uchl1* knockout mice (Figure 3E and Figure S12A) and no gross neuromuscular defect was observed at the ages tested. No significant difference in the basal pulmonary hemodynamic variables (e.g., RVSP) was observed between control and *Tie2Cre-Uchl1*$^{fl/fl}$ mice under normoxic conditions (Figure 3F and Figures S12B–E). In *Tie2Cre-Uchl1*$^{fl/fl}$ mice, hypoxia-mediated increases in RVSP, right ventricular hypertrophy (RVH) and pulmonary vascular remodeling (e.g., PA wall thickness), were significantly attenuated despite 4-weeks of hypoxia exposure compared with control mice (Figures 3F–H and Figures S12B–I). Echocardiography also confirmed that the ratio of pulmonary acceleration over ejection time (PAT/PET) is lower in wild-type (WT) mice exposed to 4 weeks of hypoxia versus those exposed to normoxia (Figure 3G and Figure S13). In contrast, *Tie2Cre-Uchl1*$^{fl/fl}$ mice exhibited increases in both, PAT values as well as the ratio of PAT/PET compared to WT mice when exposed to hypoxia (Figure 3G).

Linkage-specific UCHL1 activity and Akt1.

Based on the previously suggested role for UCHL1 in Akt1 proteasomal degradation, Akt1 ubiquitination was evaluated using a co-IP assay between ubiquitin and Akt1 in HPAECs and in rat lung tissues. Our hypothesis predicted elevated ubiquitinated Akt1 levels in mice exposed to reduced Uchl1 suggesting reduced deubiquitination. To test this hypothesis, linkage-specific modification of Akt1 ubiquitination by lysine 48 (K48) and K63 were assessed. Protein ubiquitination has been described to serve a variety of functions based on linkage-specific modifications with K48 associated with protein degradation and K63 associated with protein activation. Immunoblot results revealed reduced total K48-linked protein levels in PAECs isolated from MCT- and hypoxia-sugen-exposed rats compared to those from vehicle (Figure 4A, Figure S14A), suggesting increased proteasomal degradation of total proteins during PAH development. Immunoblot results also revealed increased K48-linked protein levels in whole lung homogenates from *Uchl1*$^{-/-}$ rats compared to those from WT with MCT exposure (Figure 4B). This trend was also observed in vehicle-exposed rats but was not statistically significant.

We next examined UCHL1-silenced HPAECs, which revealed increased total K48-linked proteins (Figure 4C), further augmented by using MG132, a proteasomal inhibitor. Moreover, UCHL1-silenced HPAECs revealed increased K48-linked (Figure 4D) and reduced lysine 63 (K63)-linked Akt1 levels (Figure 4E) in co-IP experiments. We further validated K48-linked Akt1 findings in murine PH. Specifically, hypoxic mice samples exposed to LDN57444 revealed higher K48-linked ubiquitinated Akt1 protein levels compared to those, which received vehicle (Figure S14B). These samples did not display significant differences in total loaded immunoprecipitated protein levels or in actin levels in the unbound protein. In parallel, we also observed that silencing UCHL1 resulted in greater reductions in K63-linked Akt1 activation in HPAECs derived from control cells than in those isolated from patients with PAH (Figure S14C), suggesting PAH is associated with Akt1 activation, in part, via K63-linked ubiquitination of Akt1.

Genetics and epigenetics of *UCHL1* in patients with PAH.

Based on experimental data highlighting the association of increased UCHL1 expression in PAH, we investigated the role of genetics and epigenetics in regulating *UCHL1* gene expression in patients with PAH. Specifically, review of UCSC genome browser revealed an enriched GC region in the 5’ region of the UCHL1 gene (Figure 5A), prioritizing further investigation into methylation of this region. Prior work reported rs9321, located within the 5’ UTR region of *UCHL1*, as a methylation quantitative trait locus (meQTL) in whole blood (cg15032098- β: 0.00849, SE: 0.001, P-value: 4.75×10^{-17}; cg16026922- β: 0.00896, SE: 0.0009, P-value: 1.82×10^{-23}; cg24715245- β: 0.00724, SE: 0.0007, P-value: 2.07×10^{-24}, for each copy of C (major) allele, n=5,133 subjects) [30]. Consistent with reduced methylation with the minor (T) allele, GTeX data showed association of *UCHL1* gene expression with rs9321 across several cardiovascular tissues (Figure S15A); specifically, the T allele of rs9321 was associated with increased *UCHL1* gene expression (eQTL) in lungs among other tissues relevant in PAH pathology (Figure 5B). In contrast to GTeX data, which provides observations in non-PAH lungs, we next tested the association between rs9321 and *UCHL1* gene expression levels expression to determine the same eQTL effect was observed directly in the lung tissues of patients with Group 1 PAH from genetic data available in a prior published report from the Pulmonary Hypertension Breakthrough Initiative (PHBI) cohort [20]. While not statistically significant in a smaller sample size, trends for *UCHL1* gene expression were increased with the T (minor) allele and consistent with GTeX findings (Figure S15B). Finally, we tested whether rs9321 was associated with PAH hemodynamics in patients with Group 1 PAH from the PAH Biobank. Table S3 displays basic demographics and a cohort summary. We found a significant (p value=0.024) association between rs9321 and cardiac index in an adjusted model. Each copy of the T allele decreases cardiac index by 0.2 L/min/m^2 (Figure 5C). Other hemodynamic measurements were not statistically significant (Table S4). Given these are prevalent patients with varying time between the right heart catheterization (RHC) and collection of the blood sample, we performed a sensitivity analysis where we stratified the samples by those whose duration between the two time points was less than or more than 6 months. While this association between the SNP and cardiac index was no longer significant (n=125, p0.42) in those subjects with less than 6 months duration, this analysis reduced sample size by ~85%. The association remained significant in those over 6 months (n=671, p=0.03), bolstering the importance of an adequate sample size in genetic association studies.

UCHL1 plasma levels in patients with PAH.

UCHL1 levels were measured in plasma samples from 94 Group 1 PAH patients (Table S5). In multivariable analyses adjusting for age and sex, associations between plasma levels and multiple hemodynamic measurements were significant as detailed in Table S6, suggesting an elevated UCHL1 plasma level was associated with increased PAH hemodynamic severity. Similar to the SNP association analyses, we performed a sensitivity analysis where we stratified the samples by 6 months duration between the RHC and the collection date (Tables S7 and S8). This analysis reduced sample size by nearly half per group (losing one sample due to missing information on date of RHC) and associations between plasma levels and several hemodynamics parameters remained significant in samples taken greater than 6 months from the collection date while similar significance was seen for cardiac index in the less than 6 months group.

Role of Gadd45α in UCHL1 expression *in vivo*.

Based on the differential methylation in patients and prior reports of GADD45α-mediated *UCHL1* promoter demethylation [27], we evaluated whether GADD45α, a well-known demethylating protein [15–18], regulates UCHL1 expression and mediates murine PH. In *Gadd45α* knockout (*Gadd45α*$^{-/-}$) mice lungs, total and activated Akt1 and UCHL1 protein levels were all reduced in normoxic samples consistent with previous reports [27]. We next evaluated the effects of chronic hypoxia exposure in *Gadd45α* deficiency. *Gadd45α*$^{-/-}$ mice exhibited sustained reductions in total and phospho-Akt as well as reduced levels of UCHL1 protein levels (Figures 6D–E). Immunohistochemistry staining of the lungs of *Gadd45α*$^{-/-}$ mice revealed reduced UCHL1 staining in the lung vasculature (Figure 6F), again predominantly in the endothelium under both normoxic and hypoxic exposure compared to WT mice.

Finally, *Gadd45α*$^{-/-}$ mice exposed to chronic hypoxia exhibited lower elevations in both RVSP and RVH compared to control mice exposed to hypoxia (Figures 6A and 6B). Consistent with these reductions in RVSP and RVH, histologic examination revealed significant improved vascular medial thickness and remodeling (Figure 6C and 6F) in hypoxia-exposed *Gadd45α*$^{-/-}$ mice compared to hypoxia-exposed WT mice.

DISCUSSION

Akt is an established mediator of cell survival and proliferation, both hallmarks of PAH pathology. Deletion of *Akt1* in mice previously demonstrated reduced hypoxic pulmonary hypertension associated with reduced PAEC and PASMC proliferation via mTOR signaling [10]. While most studies have evaluated regulation of Akt via its expression or activation, there are a paucity of investigations evaluating the degradation of Akt1 [12, 31]. To address this gap, the current study demonstrated a novel post-translational mechanism in PAH, elucidating UCHL1-mediated K48-linked deubiquitination of Akt1. Specifically, UCHL1 expression was found to be elevated in PAH and RV failure with higher plasma levels in subjects with markers of increased PAH severity. Furthermore, UCHL1 inhibition via pharmacological, genetic, or epigenetic approaches attenuated PAH development in animal models. Benefits from UCHL1 inhibition were mediated via concomitant increases in linkage-specific K48-linked and reduced K63-linked Akt1 ubiquitination, resulting in reduced total and activated Akt1 levels, respectively. Moreover, the novel associations between rs9321 and *UCHL1* gene methylation, expression, as well as right heart function in patients bolstered these experimental findings and prioritized UCHL1 as a new candidate gene in PAH. Cumulatively, these data suggest the link between endothelial UCHL1 and Akt deubiquitination as a novel therapeutic pathway for PAH.

DUBs play a critical role in the regulation of protein levels by deubiquitinating corresponding polyubiquitinated proteins. Consistent with the established function of UCHL1 as a DUB, we observed increased total Akt1 ubiquitination and reduce total Akt1 levels after UCHL1 inhibition or reduction *in vitro* in HPAECs and *in vivo*. Using

MG132 and co-IP assays, our findings suggest UCHL1 mediates Akt1 DUB activity via K48 linkage, modifying its proteasomal degradation. Moreover, reductions in UCHL1 also led to reduced phosphorylated Akt1. While some of this reduction may reflect reduced total Akt1 protein pools, lower phosphorylated Akt1 levels may also be explained, in part, by K63 linkage and the diverse roles of linkage-specific ubiquitination. Specifically, ubiquitination of proteins can regulate a host of processes beyond proteasomal degradation depending on linkage specificity [32]. For example, while K48-linked polyubiquitin chains generally target proteins for destruction by proteolysis, K63-linked chains can induce protein activation including increases in phosphorylated Akt [32–35]. We also observed reduced K63-linked Akt1 ubiquitination after silencing UCHL1, resulting in reduced phosphorylated Akt1. To explain this latter observation, changes in total Akt1 levels may have led to changes in phosphorylated Akt1 levels via availability of pool of total Akt1 protein that can be activated. Moreover, phosphorylated and pan-ubiquitinated Akt1 levels were both observed to be increased in hypoxic PH mice lungs *in the absence of LDN57444* (compared to normoxia). Whether these represent an increase in K63-linked Akt1 ubiquitination during PAH development remains unknown. Collectively, our findings suggest that UCHL1 DUB activity regulates Akt1 levels while UCHL1 blockade increases ubiquitinated Ak1, thereby decreasing its levels.

Several published reports observed epigenetic regulation and specifically, methylation of the *UCHL1* gene promoter [36, 37]. Based on our findings, rs9321 may represent a cis-meQTL and cis-eQTL for *UCHL1* methylation and expression, respectively in PAH. Furthermore, the SNP was associated with cardiac index, considered a surrogate measure of right heart function and PAH development. While there may be other critical and possibly functional SNPs within the *UCHL1* gene, the current data on this target SNP supports its role as a proxy for the proposed mechanism in the study and emphasizes the need for additional studies into UCHL1 genetics and epigenetics in PAH. These data from patients specifically support observations of UCHL1 expression and potential roles in both, lung vascular and RV tissues in PAH. A key limitation of these patient-level data is that all of the cohorts presented in the current work were collected as part of registries with patients predominantly with prevalent and not incident disease. Therefore, the time of assessment and progression of disease may influence the associations along with a host of confounders not available for evaluation such as socioeconomic data, medication use and compliance, among others. The rare nature of the disease increases the difficulty of accumulating a sufficiently large sample size of incident disease for genetic and biomarker associations. Nonetheless, the PAH Biobank reflects the world's largest genetic database combined with a registry for PAH and represents a powerful tool for these types of analyses as previously reported[5, 6]. They also corroborate our experimental and animal data suggesting a pathological role for UCHL1 in PAH.

Supporting potential pathologic roles for GADD45α and UCHL1, the current work observed increased expression of both proteins in PAH tissues. We also confirmed that deletion of *Gadd45α* results in reductions in UCHL1 in murine PH, predominantly within the lung vasculature, providing further evidence of tissue specificity of this pathway and links to PAH relevance. Based on prior work, *Gadd45α* deletion reduced *UCHL1* expression and was associated with reduced demethylation [15] at a specific *UCHL1* promoter site in murine lungs. GADD45α is a well-known demethylating agent [15–17], and, via orthologous gene expression profiling, *GADD45α* was identified as a highly differentially expressed gene induced by several acute and chronic lung injury stimuli [15, 27, 38, 39]. Combined with the current findings, *GADD45α* is a novel mediator of UCHL1 expression and may also represent a new remodeling target in PAH via epigenetics.

In addition to mediating PASMC proliferation and PAEC tube formation, UCHL1 expression is increased in PAECs of human PAH samples and histology demonstrated increased expression of UCHL1 levels in the lung and heart vasculature and in PAECs of human lungs, in particular. While *Tie2* is also not specific for only endothelial cells, *Tie2*-based conditional mice further support a critical role for endothelial *Uchl1* in the development of murine PH. UCHL1 also appears to be expressed in other vascular cells based on immunohistochemistry and systemic UCHL1 inhibition led to reduced vascular media thickness, RV hypertrophy and fibrosis in mice. While mice may not fully recapitulate human disease, they remain a powerful model to study disease mechanisms in PAH. Explanation of these observations may have resulted, in part, from potential downstream paracrine influences between EC and SMCs/cardiomyocytes as demonstrated by our co-culture data. Specifically, the Akt1 pathway is a well-known mediator of several downstream canonical pathways including mTOR signaling and PDGF production [10, 40], which, upon secretion from PAECs, may augment hyperplasia of smooth muscle cells via paracrine signaling. Alternatively, given the detection of circulating plasma levels, UCHL1 may also directly target SMC-derived mTOR and PDGF along with additional molecular mediators of PAH beyond Akt1 including TGFβ type I receptor/SMAD2 [41, 42] that are known to reduce SMC proliferation. The source and function of plasma UCHL1, however, remain unknown including whether they are derived from endothelial cells.

In summary, these data introduced the role of the GADD45α-UCHL1-Akt1 axis in PAH development (Figure S16). They shed insight into the epigenetic regulation and molecular targets of UCHL1 in PAECs, the latter regulated by intricate linkage-specific deubiquitination. Consistent with prior work that demonstrates a pathological role for murine UCHL1 deficiency resulting in degenerative changes in the central nervous system, constitutive Uchl1$^{-/-}$ rats in the current study also displayed significant motor function defects which were not seen in conditional *Tie2Cre-Uchl1*$^{fl/f}$ mice. While pharmacological targeting of UCHL1 will need to incorporate cell-specific delivery systems to reduce toxicity, the findings nonetheless suggest the deubiquitination system, in general, and endothelial UCHL1, more specifically, as novel therapeutic targets in PAH development.

Supplementary Material

Refer to Web version on PubMed Central for supplementary material.

FUNDING SOURCES

This study was funded by National Key Research and Development Program of China (2019YFE0119400), Natural Science Foundation of China (82370060, 81970052 and 82170057), NIH NHLBI Grant (R01HL136603 to AAD, R01HL142638 to YL, R01HL158686 to JHK, R01HL156993 to JHK, R01 HL160941 to WCN. and AAD, R24 HL105333 (MWP. and WCN), American Heart Association (AHA) (14CRP18910051 to AAD), and the American Thoracic Society Foundation/Pulmonary Hypertension Association (AAD), Veterans Administration

Health System (BX006003 to LH), and the Open Project of State Key Laboratory of Respiratory Disease (SKLRD-OP-202114/202301).

REFERENCES

1. Pauwaa S, Machado RF and Desai AA. Survival in pulmonary arterial hypertension: A brief review of registry data. Pulm Circ. 2011;1:430–1. [PubMed: 22140634]
2. Benza RL, Gomberg-Maitland M, Miller DP, Frost A, Frantz RP, Foreman AJ, Badesch DB and McGoon MD. The REVEAL Registry risk score calculator in patients newly diagnosed with pulmonary arterial hypertension. Chest. 2012;141:354–62. [PubMed: 21680644]
3. McLaughlin VV, Archer SL, Badesch DB, Barst RJ, Farber HW, Lindner JR, Mathier MA, McGoon MD, Park MH, Rosenson RS, Rubin LJ, Tapson VF, Varga J, Harrington RA, Anderson JL, Bates ER, Bridges CR, Eisenberg MJ, Ferrari VA, Grines CL, Hlatky MA, Jacobs AK, Kaul S, Lichtenberg RC, Moliterno DJ, Mukherjee D, Pohost GM, Schofield RS, Shubrooks SJ, Stein JH, Tracy CM, Weitz HH and Wesley DJ. ACCF/AHA 2009 expert consensus document on pulmonary hypertension: a report of the American College of Cardiology Foundation Task Force on Expert Consensus Documents and the American Heart Association: developed in collaboration with the American College of Chest Physicians, American Thoracic Society, Inc., and the Pulmonary Hypertension Association. Circulation. 2009;119:2250–94. [PubMed: 19332472]
4. Wilkins MR. Pulmonary hypertension: the science behind the disease spectrum. Eur Respir Rev. 2012;21:19–26. [PubMed: 22379170]
5. Rhodes CJ, Batai K, Bleda M, Haimel M, Southgate L, Germain M, Pauciulo MW, Hadinnapola C, Aman J, Girerd B, Arora A, Knight J, Hanscombe KB, Karnes JH, Kaakinen M, Gall H, Ulrich A, Harbaum L, Cebola I, Ferrer J, Lutz K, Swietlik EM, Ahmad F, Amouyel P, Archer SL, Argula R, Austin ED, Badesch D, Bakshi S, Barnett C, Benza R, Bhatt N, Bogaard HJ, Burger CD, Chakinala M, Church C, Coghlan JG, Condliffe R, Corris PA, Danesino C, Debette S, Elliott CG, Elwing J, Eyries M, Fortin T, Franke A, Frantz RP, Frost A, Garcia JGN, Ghio S, Ghofrani HA, Gibbs JSR, Harley J, He H, Hill NS, Hirsch R, Houweling AC, Howard LS, Ivy D, Kiely DG, Klinger J, Kovacs G, Lahm T, Laudes M, Machado RD, Ross RVM, Marsolo K, Martin LJ, Moledina S, Montani D, Nathan SD, Newnham M, Olschewski A, Olschewski H, Oudiz RJ, Ouwehand WH, Peacock AJ, Pepke-Zaba J, Rehman Z, Robbins I, Roden DM, Rosenzweig EB, Saydain G, Scelsi L, Schilz R, Seeger W, Shaffer CM, Simms RW, Simon M, Sitbon O, Suntharalingam J, Tang H, Tchourbanov AY, Thenappan T, Torres F, Toshner MR, Treacy CM, Vonk Noordegraaf A, Waisfisz Q, Walsworth AK, Walter RE, Wharton J, White RJ, Wilt J, Wort SJ, Yung D, Lawrie A, Humbert M, Soubrier F, Tregouet DA, Prokopenko I, Kittles R, Graf S, Nichols WC, Trembath RC, Desai AA, Morrell NW, Wilkins MR, Consortium UNBRD, Consortium UPCS and Consortium UPB. Genetic determinants of risk in pulmonary arterial hypertension: international genome-wide association studies and meta-analysis. Lancet Respir Med. 2018.
6. Sangam S, Sun X, Schwantes-An TH, Yegambaram M, Lu Q, Shi Y, Cook T, Fisher A, Frump AL, Coleman A, Sun Y, Liang S, Crawford H, Lutz KA, Maun AD, Pauciulo MW, Karnes JH, Chaudhary KR, Stewart DJ, Langlais PR, Jain M, Alotaibi M, Lahm T, Jin Y, Gu H, Tang H, Nichols WC, Black SM and Desai AA. SOX17 Deficiency Mediates Pulmonary Hypertension: At the Crossroads of Sex, Metabolism, and Genetics. Am J Respir Crit Care Med. 2023.
7. Guignabert C, Tu L, Le Hiress M, Ricard N, Sattler C, Seferian A, Huertas A, Humbert M and Montani D. Pathogenesis of pulmonary arterial hypertension: lessons from cancer. Eur Respir Rev. 2013;22:543–51. [PubMed: 24293470]
8. Maron BA and Loscalzo J. Pulmonary hypertension: pathophysiology and signaling pathways. Handbook of experimental pharmacology. 2013;218:31–58. [PubMed: 24092335]
9. Meloche J, Pflieger A, Vaillancourt M, Paulin R, Potus F, Zervopoulos S, Graydon C, Courboulin A, Breuils-Bonnet S, Tremblay E, Couture C, Michelakis ED, Provencher S and Bonnet S. Role for DNA damage signaling in pulmonary arterial hypertension. Circulation. 2014;129:786–97. [PubMed: 24270264]
10. Tang H, Chen J, Fraidenburg DR, Song S, Sysol JR, Drennan AR, Offermanns S, Ye RD, Bonini MG, Minshall RD, Garcia JG, Machado RF, Makino A and Yuan JX. Deficiency of Akt1, but not Akt2, attenuates the development of pulmonary hypertension. Am J Physiol Lung Cell Mol Physiol. 2015;308:L208–20. [PubMed: 25416384]

11. Tang H, Wu K, Wang J, Vinjamuri S, Gu Y, Song S, Wang Z, Zhang Q, Balistrieri A, Ayon RJ, Rischard F, Vanderpool R, Chen J, Zhou G, Desai AA, Black SM, Garcia JGN, Yuan JX and Makino A. Pathogenic Role of mTORC1 and mTORC2 in Pulmonary Hypertension. JACC Basic Transl Sci. 2018;3:744–762. [PubMed: 30623134]
12. Chan CH, Jo U, Kohrman A, Rezaeian AH, Chou PC, Logothetis C and Lin HK. Posttranslational regulation of Akt in human cancer. Cell Biosci. 2014;4:59. [PubMed: 25309720]
13. Yang WL, Wu CY, Wu J and Lin HK. Regulation of Akt signaling activation by ubiquitination. Cell Cycle. 2010;9:487–97. [PubMed: 20081374]
14. Shi Y, Gu C, Zhao T, Jia Y, Bao C, Luo A, Guo Q, Han Y, Wang J, Black SM, Desai AA and Tang H. Combination Therapy With Rapamycin and Low Dose Imatinib in Pulmonary Hypertension. Front Pharmacol. 2021;12:758763. [PubMed: 34858182]
15. Mitra S, Sammani S, Wang T, Boone DL, Meyer NJ, Dudek SM, Moreno-Vinasco L, Garcia JG and Jacobson JR. Role of growth arrest and DNA damage-inducible alpha in Akt phosphorylation and ubiquitination after mechanical stress-induced vascular injury. Am J Respir Crit Care Med. 2011;184:1030–40. [PubMed: 21816939]
16. Barreto G, Schafer A, Marhold J, Stach D, Swaminathan SK, Handa V, Doderlein G, Maltry N, Wu W, Lyko F and Niehrs C. Gadd45a promotes epigenetic gene activation by repair-mediated DNA demethylation. Nature. 2007;445:671–5. [PubMed: 17268471]
17. Cortellino S, Xu J, Sannai M, Moore R, Caretti E, Cigliano A, Le Coz M, Devarajan K, Wessels A, Soprano D, Abramowitz LK, Bartolomei MS, Rambow F, Bassi MR, Bruno T, Fanciulli M, Renner C, Klein-Szanto AJ, Matsumoto Y, Kobi D, Davidson I, Alberti C, Larue L and Bellacosa A. Thymine DNA glycosylase is essential for active DNA demethylation by linked deamination-base excision repair. Cell. 2011;146:67–79. [PubMed: 21722948]
18. Arab K, Karaulanov E, Musheev M, Trnka P, Schafer A, Grummt I and Niehrs C. GADD45A binds R-loops and recruits TET1 to CpG island promoters. Nat Genet. 2019;51:217–223. [PubMed: 30617255]
19. Zhu N, Pauciulo MW, Welch CL, Lutz KA, Coleman AW, Gonzaga-Jauregui C, Wang J, Grimes JM, Martin LJ, He H, Investigators PAHBEC, Shen Y, Chung WK and Nichols WC. Novel risk genes and mechanisms implicated by exome sequencing of 2572 individuals with pulmonary arterial hypertension. Genome Med. 2019;11:69. [PubMed: 31727138]
20. Stearman RS, Bui QM, Speyer G, Handen A, Cornelius AR, Graham BB, Kim S, Mickler EA, Tuder RM, Chan SY and Geraci MW. Systems Analysis of the Human Pulmonary Arterial Hypertension Lung Transcriptome. Am J Respir Cell Mol Biol. 2019;60:637–649. [PubMed: 30562042]
21. Omura J, Habbout K, Shimauchi T, Wu WH, Breuils-Bonnet S, Tremblay E, Martineau S, Nadeau V, Gagnon K, Mazoyer F, Perron J, Potus F, Lin JH, Zafar H, Kiely DG, Lawrie A, Archer SL, Paulin R, Provencher S, Boucherat O and Bonnet S. Identification of Long Noncoding RNA H19 as a New Biomarker and Therapeutic Target in Right Ventricular Failure in Pulmonary Arterial Hypertension. Circulation. 2020;142:1464–1484. [PubMed: 32698630]
22. Tang H, Babicheva A, McDermott KM, Gu Y, Ayon RJ, Song S, Wang Z, Gupta A, Zhou T, Sun X, Dash S, Wang Z, Balistrieri A, Zheng Q, Cordery AG, Desai AA, Rischard F, Khalpey Z, Wang J, Black SM, Garcia JGN, Makino A and Yuan JX. Endothelial HIF-2alpha contributes to severe pulmonary hypertension due to endothelial-to-mesenchymal transition. Am J Physiol Lung Cell Mol Physiol. 2018;314:L256–L275. [PubMed: 29074488]
23. Tang H, Yamamura A, Yamamura H, Song S, Fraidenburg DR, Chen J, Gu Y, Pohl NM, Zhou T, Jimenez-Perez L, Ayon RJ, Desai AA, Goltzman D, Rischard F, Khalpey ZI, Black SM, Garcia JG, Makino A and Yuan JX. Pathogenic Role of Calcium-sensing Receptors in the Development and Progression of Pulmonary Hypertension. Am J Physiol Lung Cell Mol Physiol. 2016:ajplung 00050 2016.
24. Chen F, Sugiura Y, Myers KG, Liu Y and Lin W. Ubiquitin carboxyl-terminal hydrolase L1 is required for maintaining the structure and function of the neuromuscular junction. Proc Natl Acad Sci U S A. 2010;107:1636–41. [PubMed: 20080621]
25. Sakurai M, Sekiguchi M, Zushida K, Yamada K, Nagamine S, Kabuta T and Wada K. Reduction in memory in passive avoidance learning, exploratory behaviour and synaptic plasticity in mice

with a spontaneous deletion in the ubiquitin C-terminal hydrolase L1 gene. Eur J Neurosci. 2008;27:691–701. [PubMed: 18279321]

26. Setsuie R, Wang YL, Mochizuki H, Osaka H, Hayakawa H, Ichihara N, Li H, Furuta A, Sano Y, Sun YJ, Kwon J, Kabuta T, Yoshimi K, Aoki S, Mizuno Y, Noda M and Wada K. Dopaminergic neuronal loss in transgenic mice expressing the Parkinson's disease-associated UCH-L1 I93M mutant. Neurochem Int. 2007;50:119–29. [PubMed: 16965839]
27. Meyer NJ, Huang Y, Singleton PA, Sammani S, Moitra J, Evenoski CL, Husain AN, Mitra S, Moreno-Vinasco L, Jacobson JR, Lussier YA and Garcia JG. GADD45a is a novel candidate gene in inflammatory lung injury via influences on Akt signaling. FASEB J. 2009;23:1325–37. [PubMed: 19124556]
28. Mi Z, Liu H, Rose ME, Ma X, Reay DP, Ma J, Henchir J, Dixon CE and Graham SH. Abolishing UCHL1's hydrolase activity exacerbates TBI-induced axonal injury and neuronal death in mice. Exp Neurol. 2021;336:113524. [PubMed: 33159930]
29. Saigoh K, Wang YL, Suh JG, Yamanishi T, Sakai Y, Kiyosawa H, Harada T, Ichihara N, Wakana S, Kikuchi T and Wada K. Intragenic deletion in the gene encoding ubiquitin carboxy-terminal hydrolase in gad mice. Nat Genet. 1999;23:47–51. [PubMed: 10471497]
30. Huan T, Joehanes R, Song C, Peng F, Guo Y, Mendelson M, Yao C, Liu C, Ma J, Richard M, Agha G, Guan W, Almli LM, Conneely KN, Keefe J, Hwang SJ, Johnson AD, Fornage M, Liang L and Levy D. Genome-wide identification of DNA methylation QTLs in whole blood highlights pathways for cardiovascular disease. Nat Commun. 2019;10:4267. [PubMed: 31537805]
31. Dienstmann R, Rodon J, Serra V and Tabernero J. Picking the point of inhibition: a comparative review of PI3K/AKT/mTOR pathway inhibitors. Mol Cancer Ther. 2014;13:1021–31. [PubMed: 24748656]
32. Komander D, Clague MJ and Urbe S. Breaking the chains: structure and function of the deubiquitinases. Nat Rev Mol Cell Biol. 2009;10:550–63. [PubMed: 19626045]
33. Lim JH, Jono H, Komatsu K, Woo CH, Lee J, Miyata M, Matsuno T, Xu X, Huang Y, Zhang W, Park SH, Kim YI, Choi YD, Shen H, Heo KS, Xu H, Bourne P, Koga T, Xu H, Yan C, Wang B, Chen LF, Feng XH and Li JD. CYLD negatively regulates transforming growth factor-beta-signalling via deubiquitinating Akt. Nat Commun. 2012;3:771. [PubMed: 22491319]
34. Yang WL, Jin G, Li CF, Jeong YS, Moten A, Xu D, Feng Z, Chen W, Cai Z, Darnay B, Gu W and Lin HK. Cycles of ubiquitination and deubiquitination critically regulate growth factor-mediated activation of Akt signaling. Sci Signal. 2013;6:ra3. [PubMed: 23300340]
35. Yang WL, Wang J, Chan CH, Lee SW, Campos AD, Lamothe B, Hur L, Grabiner BC, Lin X, Darnay BG and Lin HK. The E3 ligase TRAF6 regulates Akt ubiquitination and activation. Science. 2009;325:1134–8. [PubMed: 19713527]
36. Kleiman DA, Beninato T, Sultan S, Crowley MJ, Finnerty B, Kumar R, Panarelli NC, Liu YF, Lieberman MD, Seandel M, Evans T, Elemento O, Zarnegar R and Fahey TJ, 3rd. Silencing of UCHL1 by CpG promoter hyper-methylation is associated with metastatic gastroenteropancreatic well-differentiated neuroendocrine (carcinoid) tumors. Ann Surg Oncol. 2014;21 Suppl 4:S672–9. [PubMed: 24854489]
37. Mandelker DL, Yamashita K, Tokumaru Y, Mimori K, Howard DL, Tanaka Y, Carvalho AL, Jiang WW, Park HL, Kim MS, Osada M, Mori M and Sidransky D. PGP9.5 promoter methylation is an independent prognostic factor for esophageal squamous cell carcinoma. Cancer research. 2005;65:4963–8. [PubMed: 15930319]
38. Mathew B, Takekoshi D, Sammani S, Epshtein Y, Sharma R, Smith BD, Mitra S, Desai AA, Weichselbaum RR, Garcia JG and Jacobson JR. Role of GADD45a in murine models of radiation- and bleomycin-induced lung injury. Am J Physiol Lung Cell Mol Physiol. 2015;309:L1420–9. [PubMed: 26498248]
39. Mitra S, Wade MS, Sun X, Moldobaeva N, Flores C, Ma SF, Zhang W, Garcia JG and Jacobson JR. GADD45a promoter regulation by a functional genetic variant associated with acute lung injury. PLoS One. 2014;9:e100169. [PubMed: 24940746]
40. Chen H, Guan R, Lei Y, Chen J, Ge Q, Zhang X, Dou R, Chen H, Liu H, Qi X, Zhou X and Chen C. Lymphangiogenesis in gastric cancer regulated through Akt/mTOR-VEGF-C/VEGF-D axis. BMC Cancer. 2015;15:103. [PubMed: 25884175]

41. Liu S, Gonzalez-Prieto R, Zhang M, Geurink PP, Kooij R, Iyengar PV, van Dinther M, Bos E, Zhang X, Le Devedec SE, van de Water B, Koning RI, Zhu HJ, Mesker WE, Vertegaal ACO, Ovaa H, Zhang L, Martens JWM and Ten Dijke P. Deubiquitinase Activity Profiling Identifies UCHL1 as a Candidate Oncoprotein That Promotes TGFbeta-Induced Breast Cancer Metastasis. Clin Cancer Res. 2020;26:1460–1473. [PubMed: 31857432]
42. Xia X, Xu Q, Liu M, Chen X, Liu X, He J, Hu T, Yu C, Huang H, Liu S and Liu N. Deubiquitination of CD36 by UCHL1 promotes foam cell formation. Cell Death Dis. 2020;11:636. [PubMed: 32801299]
43. Moreno-Vinasco L, Gomberg-Maitland M, Maitland ML, Desai AA, Singleton PA, Sammani S, Sam L, Liu Y, Husain AN, Lang RM, Ratain MJ, Lussier YA and Garcia JG. Genomic assessment of a multikinase inhibitor, sorafenib, in a rodent model of pulmonary hypertension. Physiol Genomics. 2008;33:278–91. [PubMed: 18303084]
44. Tang H, Yamamura A, Yamamura H, Song S, Fraidenburg DR, Chen J, Gu Y, Pohl NM, Zhou T, Jimenez-Perez L, Ayon RJ, Desai AA, Goltzman D, Rischard F, Khalpey Z, Black SM, Garcia JG, Makino A and Yuan JX. Pathogenic role of calcium-sensing receptors in the development and progression of pulmonary hypertension. Am J Physiol Lung Cell Mol Physiol. 2016;310:L846–59. [PubMed: 26968768]
45. Anderson KR, Haeussler M, Watanabe C, Janakiraman V, Lund J, Modrusan Z, Stinson J, Bei Q, Buechler A, Yu C, Thamminana SR, Tam L, Sowick MA, Alcantar T, O'Neil N, Li J, Ta L, Lima L, Roose-Girma M, Rairdan X, Durinck S and Warming S. CRISPR off-target analysis in genetically engineered rats and mice. Nat Methods. 2018;15:512–514. [PubMed: 29786090]

Significance Statement:

We present a novel role for a well-established deubiquitinase, UCHL1, in the development of PAH.

Clinical Perspective:

What is new?

a. Using cell culture, animal models, and multi-omics patient-level data, we present the first evidence of the pathological role of an enzyme responsible for deubiquitination of proteins in endothelial cells which contributes to the development of PAH.

b. While inhibiting the activation of Akt1 has been well-studied in PAH, this work suggests that Akt1 degradation may also be a novel mechanism that contributes to PAH development.

What are the clinical implications?

a. The current work demonstrates that endothelial UCHL1 plays a critical role in PAH development and targeting deubiquitinases may be a novel therapeutic pathway in PAH.

b. The work also underscores the prospect of targeting Akt1 for proteasomal degradation as a potential therapeutic strategy in PAH.

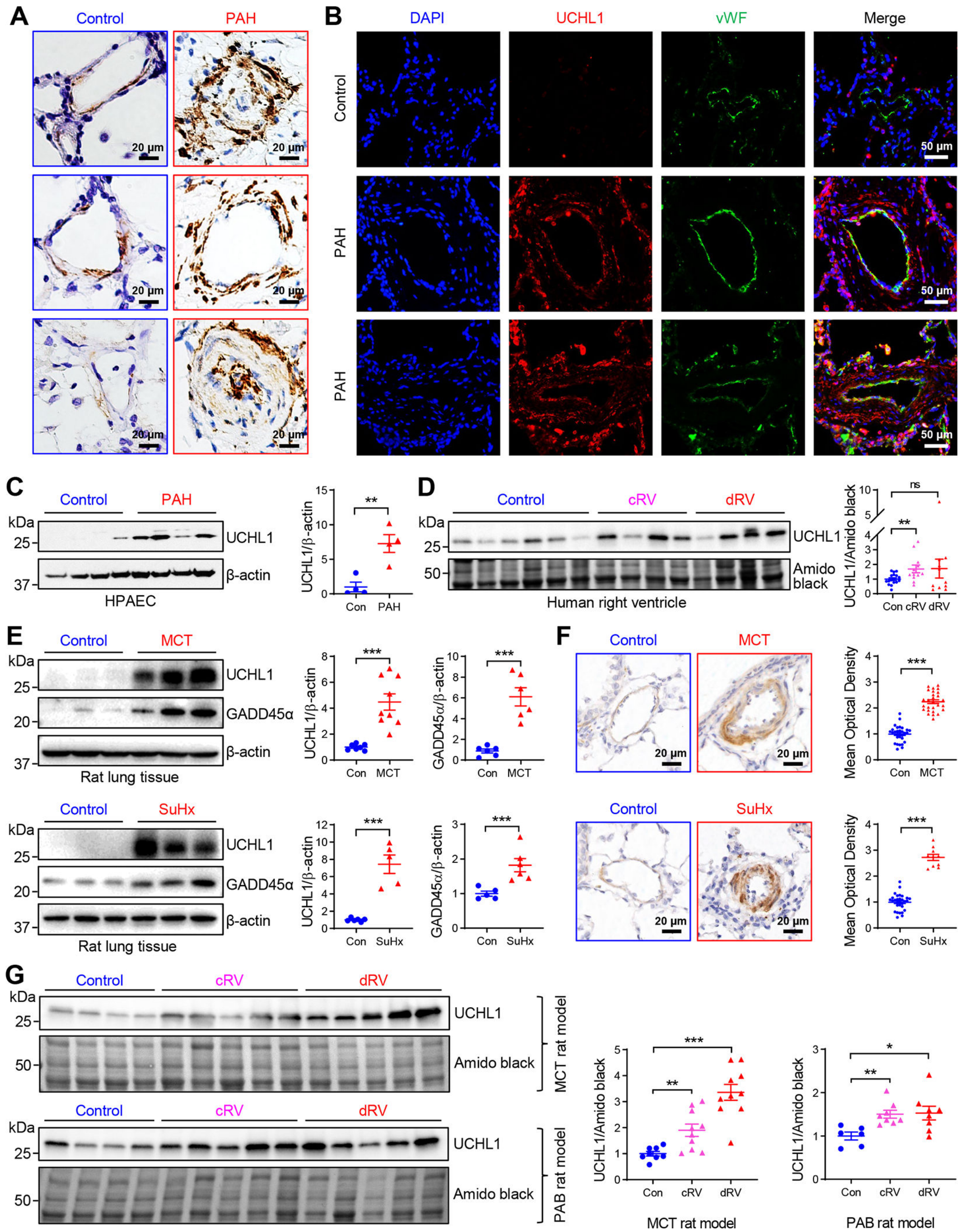

Figure 1. Elevated UCHL1 expression in PAH.

A) Immunohistochemistry (IHC) reveals increased vascular-specific staining of UCHL1 in patients with PAH (n=3) compared to control patients (n=3). **B)** Immunofluorescence reveals co-localization of UCHL1 staining with vWF$^+$ cells, consistent with increased expression in HPAECs (n=3). **C)** UCHL1 protein levels are higher in HPAECs isolated from subjects with PAH (n=5) than from controls (n=4). **D)** UCHL1 protein levels are higher in RV tissues isolated from subjects with RV hypertrophy (compensated RV or cRV with n=12 and decompensated RV or dRV with n=11) than from controls (n=17). **E)** Western blots demonstrate increased UCHL1 and GADD45α levels in MCT-exposed rats and in SuHx-exposed rats compared to their respective controls. **F)** IHC display increased UCHL1 staining in MCT-exposed rats and SuHx-exposed rats compared to their respective controls. **G)** UCHL1 protein levels are higher in RV tissues isolated from MCT-exposed rats (cRV and dRV, n=20 total) than from controls (n=10) and from PAB-exposed rats (cRV and dRV with n=17 total) than from controls (n=7). *p≤0.05, **p<0.01, ***p<0.001

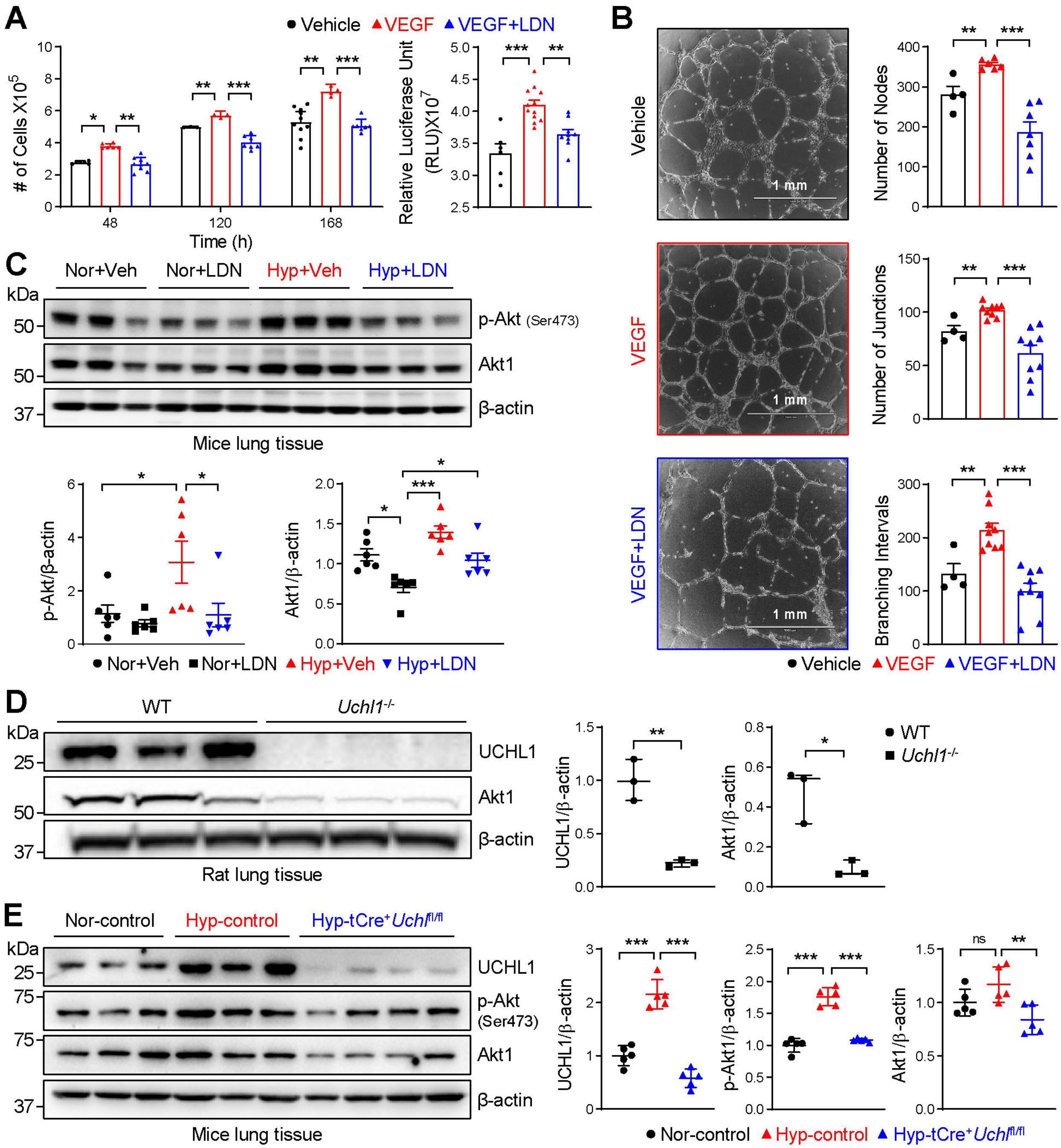

Figure 2. UCHL1 inhibition reduces PAEC proliferation, tube formation, and Akt1 levels.
A) After VEGF administration (10 ng/mL), quantitative measurements of cell counts reveal reduced HPAEC proliferation over time with co-administration of LDN57444. BrdU incorporation assay reveals reduced cell proliferation *in vitro* with co-administration of LDN57444 in HPAECs exposed to VEGF. **B)** Using a tube formation assay, HPAECs exposed to LDN57444 exhibited significantly suppressed VEGF-induced tube formation due to formation of lower numbers of node, junction, and intervals observed in 3D culture. **C)** While total Akt1 levels rise mildly, hypoxia exposure significantly upregulates phospho-Akt

protein levels in mouse lungs of WT mice. With LDN57444 administration, both total and phospho-Akt protein levels are reduced. **D)** *Uchl1*$^{-/-}$ rats demonstrate reduced p-Akt1 and slightly reduced total Akt1 levels in whole lung homogenates than WT. **E)** *Tie2Cre-Uchl1*$^{fl/fl}$ mice displayed reduced UCHL1, p-Akt1 and slightly reduced total Akt1 levels in whole lung homogenates compared to cage controls. The numbers of experiments (n) for each group are indicated in each bar. Analysis of variance, *p≤0.05, **p<0.01, ***p<0.001

Author Manuscript
Author Manuscript
Author Manuscript

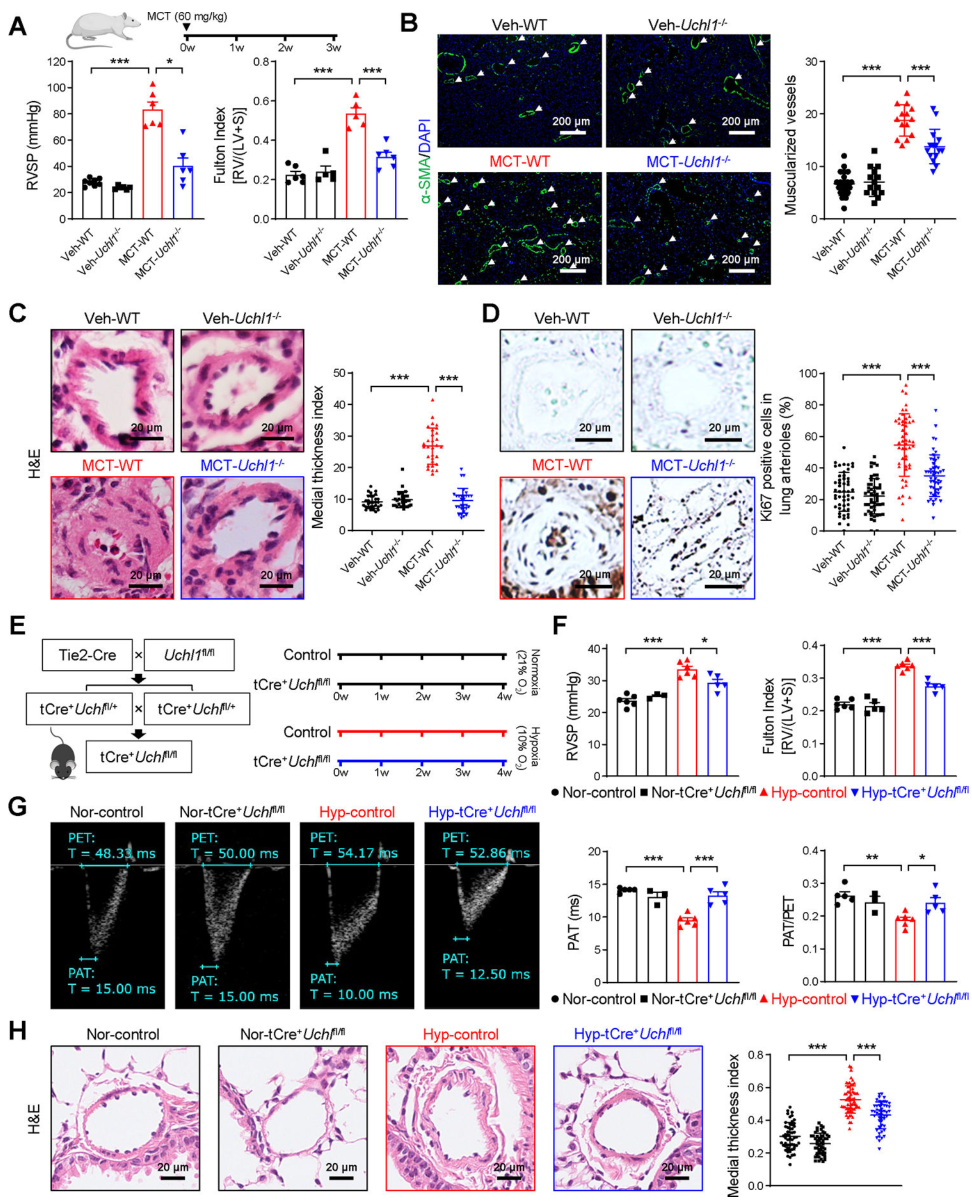

Figure 3. *Uchl1* deletion attenuates animal PH.

Rats with *Uchl1* deletion resulted in reduced **A**) RVSP (Veh-WT: 27.0 α 1.0, Veh-*Uchl1*$^{-/-}$: 23.9 α 0.6, MCT-WT: 83.6 α 5.6, MCT-*Uchl1*$^{-/-}$: 40.4 α 6.1 mm Hg), and RVH (Veh-WT: 0.23 α 0.02, Veh-*Uchl1*$^{-/-}$: 0.24 α 0.03, MCT-WT: 0.53 α 0.03, MCT-*Uchl1*$^{-/-}$: 0.32 α 0.02), **B and C)** pulmonary artery medial histology and thickness, muscularized vessel counts and staining, as well as **D)** ki-67 staining in rat lungs compared to WT after exposure to MCT. **E**) Schematic strategy for the generation of *Tie2Cre-Uchl1*$^{fl/fl}$ mice and modeling in hypoxia. **F)** Summarized data showing RVSP and the Fulton index in control and *Tie2Cre-Uchl1*$^{fl/fl}$ mice exposed to normoxia and hypoxia. **G)** Representative images of pulmonary outflow pulse wave Doppler tracing and summarized data of echocardiography showing pulmonary acceleration time divided by pulmonary ejection time (PAT/PET ratios). **H)** Representative histology images of small PA and summarized data showing

PA wall thickness in cage control and *Tie2Cre-Uchl1*$^{fl/fl}$ mice under normoxic and hypoxic conditions. Data above presented as mean ± SEM. *p≤0.05, **p<0.01, ***p<0.001. The numbers of experiments (n) for each group are indicated in each bar.

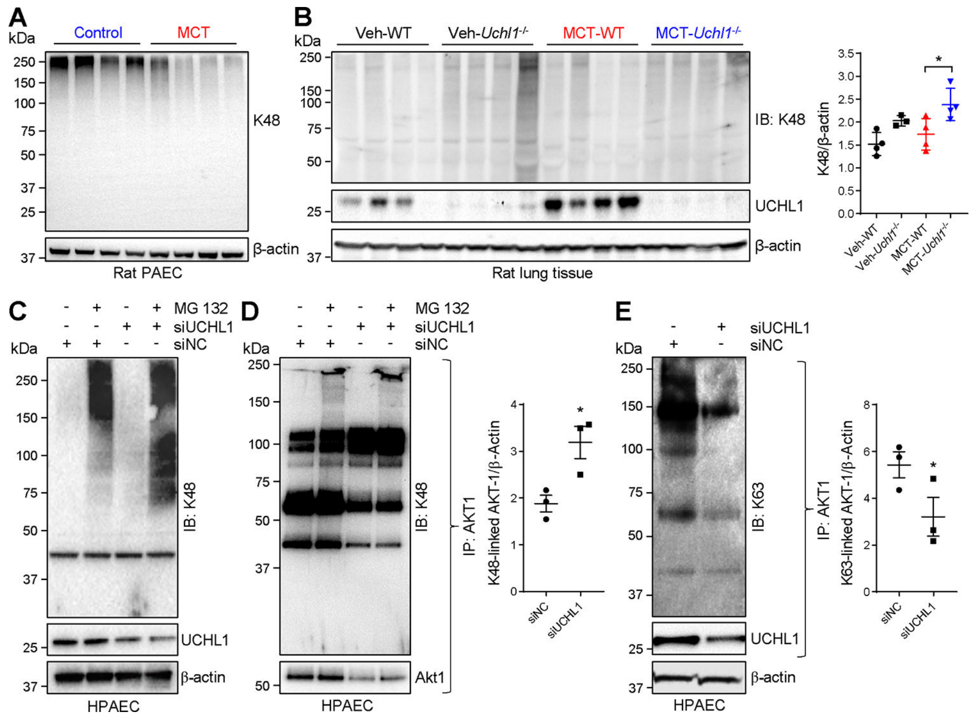

Figure 4. UCHL1-mediated linkage-specific modification of Akt1.

A) Immunoblot results revealed reduced total K48-linked protein levels in PAECs isolated from MCT-exposed rats compared to those from vehicle. **B)** Immunoblot results revealed increased K48-linked protein levels in whole lungs of *Uchl1* knockout rats compared to those from cage controls or WT rats with MCT exposure. This trend was also observed in vehicle-exposed rats but was not statistically significant. **C)** Silencing UCHL1 for 48 hours in HPAECs resulted in increased K48-linked proteins which was further increased by exposure to MG132. Silencing UCHL1 for 48 hours in HPAECs resulted in increased K48-linked Akt1 **(D)** and reduced K63-linked Akt1 levels **(E)**. Total loaded immunoprecipitated protein levels and actin levels in the unbound (to the immunoprecipitate) protein remained unchanged. * p≤0.05, **p<0.01, *** p<0.001.

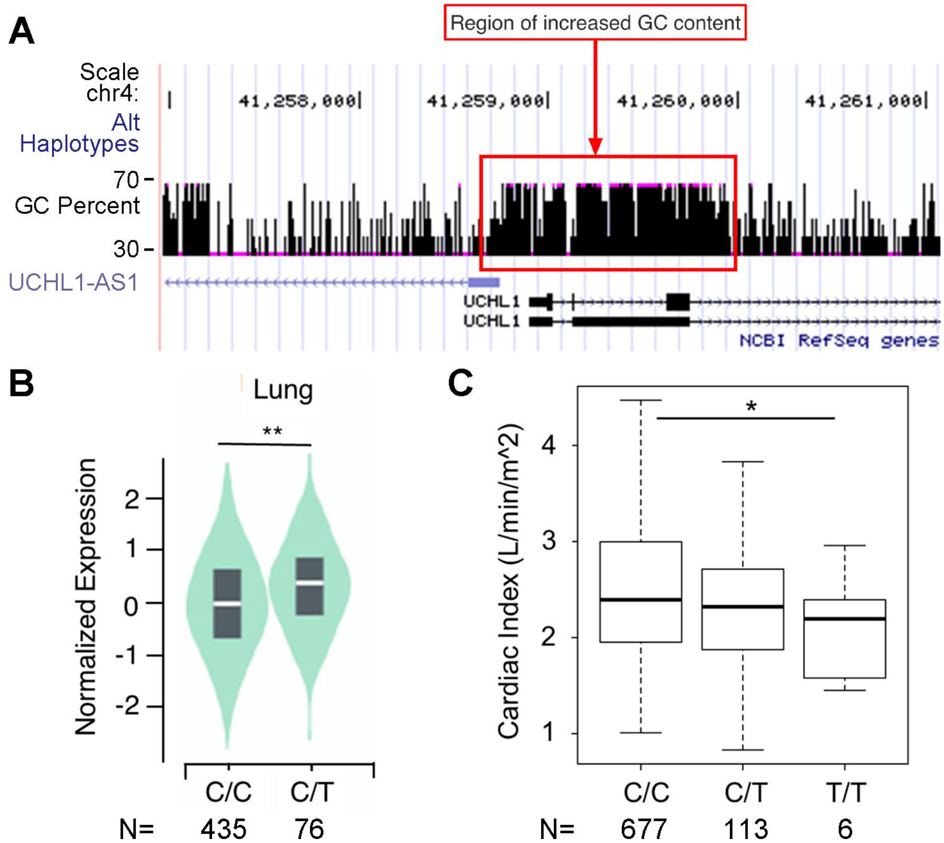

Figure 5. *UCHL1* epigenetics in patients with PAH.

A) The illustration depicts a highly GC-enriched region of the 5’ *UCHL1* gene locus; rs9321 resides in this region. **B)** Analyses of GTeX reveals cis-eQTL of rs9321 with *UCHL1* gene expression, with the T allele of associated with increased *UCHL1* gene expression in lungs ($p = 1.1 \times 10^{-8}$). **C)** Association between rs9321 and cardiac index was statistically significant ($P = 0.024$). Each copy of T allele decreases cardiac index by a Beta of 0.2.

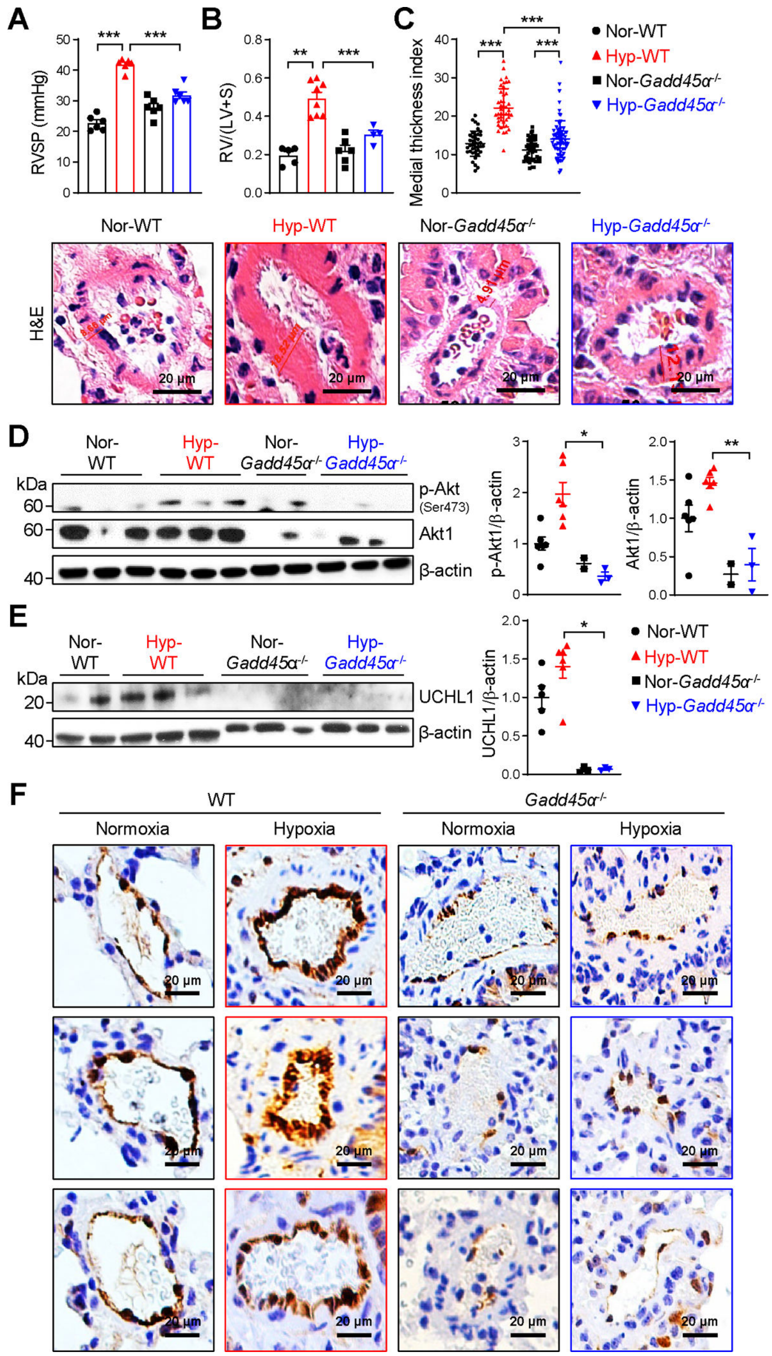

Figure 6. *Gadd45α* deletion results in attenuated murine hypoxic PH with reduced UCHL1 and Akt.

A) While both WT and *Gadd45α*$^{-/-}$ mice exhibit elevated RVSP, *Gadd45α*$^{-/-}$ mice demonstrate reduced RVSP (Nor-WT: 22.7 α 1.0, Hyp-WT: 41.8 α 0.8, Nor-*Gadd45α*$^{-/-}$: 27.9 α 1.3, Hyp-*Gadd45α*$^{-/-}$: 31.8 α 1.1 mmHg) and **B**) RVH (Nor-WT: 0.20 α 0.02, Hyp-WT: 0.49 α 0.03, Nor-*Gadd45α*$^{-/-}$: 0.22 α 0.03, Hyp-*Gadd45α*$^{-/-}$: 0.30 α 0.02) compared to WT mice when exposed to hypoxia. Data presented as mean ± SEM. The numbers of experiments (n) for each group are indicated in each bar. **C)** While both

WT and *Gadd45α*$^{-/-}$ mice develop vascular remodeling after exposure to hypoxic PH, *Gadd45α*$^{-/-}$ mice demonstrate reduced pulmonary artery medial thickness index compared to WT mice hypoxic lungs. **D)** Hypoxia exposure upregulates total and phospho-Akt protein levels in whole mouse lung homogenates of WT mice. With *Gadd45α* deficiency, both total and phospho-Akt protein levels are reduced. **E)** Western blot from lung homogenates from wild type and *Gadd45α*$^{-/-}$ mice show reduced expression of UCHL1 protein. **F)** Immunohistochemistry reveals increased UCHL1 staining in WT mice exposed to chronic hypoxia compared to normoxia mice, which appears to be predominantly within the endothelium. $^{*}p \leq 0.05$, $^{**}p < 0.01$, $^{***}p < 0.001$.